Dark Solar Wind

Jae Hyeok Chang[1,2,*] David E. Kaplan,[1,†] Surjeet Rajendran,[1,‡] Harikrishnan Ramani,[3,§] and Erwin H. Tanin[1,‖]

[1]*Department of Physics and Astronomy, Johns Hopkins University, Baltimore, Maryland 21218, USA*
[2]*Maryland Center for Fundamental Physics, Department of Physics, University of Maryland, College Park, Maryland 20742, USA*
[3]*Stanford Institute for Theoretical Physics, Stanford University, Stanford, California 94305, USA*

We study the solar emission of light dark sector particles that self-interact strongly enough to self-thermalize. The resulting outflow behaves like a fluid which accelerates under its own thermal pressure to highly relativistic bulk velocities in the solar system. Compared to the ordinary noninteracting scenario, the local outflow has at least $\sim 10^3$ higher number density and correspondingly at least $\sim 10^3$ lower average energy per particle. We show how this generic phenomenon arises in a dark sector composed of millicharged particles strongly self-interacting via a dark photon. The millicharged plasma wind emerging in this model has novel yet predictive signatures that encourages new experimental directions. This phenomenon demonstrates how a small step away from the simplest models can lead to radically different outcomes and thus motivates a broader search for dark sector particles.

Light particles with some coupling to the standard model (SM) can be produced in the Sun with $\sim$keV energies. The luminosity of such particles is strongly limited by stellar cooling arguments [1]. If these particles simply free stream away as soon as they are produced in the Sun, the outcome is an outflow of $\sim$keV energy particles whose particle-number flux is currently too low to be detected near Earth. However, interactions within the dark sector are in general poorly constrained, and, as we will show, the story can change dramatically if one takes them into account.

We focus on the predictive scenario where the interactions within the dark sector allow these particles to locally thermalize via number-changing processes. There are two natural outcomes of this scenario. (1) While the dark-particle luminosity is still limited by cooling bounds, the self-thermalization of these particles has the effect of enhancing the resulting particle-number flux at the expense of lowering the average energy per particle. Furthermore, (2) once local thermal equilibrium can be established, the mean free path of these particles can be microscopically small and on macroscopic scales they collectively display hydrodynamic behavior which further modifies the properties of the outflow. The actual dynamics is a mixture of both effects and this gives rise to novel experimental and astrophysical signatures.

As long as these particles are relativistic, their thermal pressure will continually convert thermal energy into bulk fluid motion. In a way mathematically analogous to the Parker solar wind model [2], this eventually leads to a steady outflow of the fast dark-particle fluid, which we refer to as the *dark solar wind*.

We elaborate these points in the remainder of this Letter. For concreteness, we adopt a model of dark fermions interacting via dark photons as a representative of a self-interacting dark sector. In order to have this sector produced in the Sun, the dark photon is assumed to have a small kinetic mixing with the SM photon [3], thus making the dark fermions effectively millicharged. This property also enables this dark solar wind to be detectable on Earth.

Model.—Our Lagrangian is described by

$$\mathcal{L}_D = -\frac{1}{4}F'_{\mu\nu}F'^{\mu\nu} - \frac{\epsilon}{2}F'_{\mu\nu}F^{\mu\nu} + \bar{\chi}(i\gamma^\mu\partial_\mu + g_D\gamma^\mu A'_\mu - m_\chi)\chi, \qquad (1)$$

where χ is a dark fermion with mass m_χ, A' is the massless dark photon, ϵ is the mixing angle between the SM photon and the dark photon, and $g_D = \sqrt{4\pi\alpha_D}$ is the dark gauge coupling. Once the kinetic terms are diagonalized, χ is effectively millicharged and couples to the SM photon with electric charge ϵg_D. This model has been studied in various contexts (see, e.g., [4,5] for reviews), including the recent works [6–8].

In the main part of the analysis, we limit ourselves to the parameter space where m_χ is light enough that the resulting phenomenology is equivalent to that of massless fermions. We will clarify the boundary of this regime and comment on how the phenomenology would change for heavier m_χ.

Production in the Sun.—Because of their nonzero electric charge, χ particles can be pair created from the hot and dense SM plasma inside the Sun. For a dark fermion χ with mass much smaller than the solar temperature ($m_\chi \ll T_\odot$), the dominant production mechanism is via transverse plasmon decays. The number-density production rate $\dot{n}$ and the power per unit volume $\dot{Q}$ in the form of $\chi\bar{\chi}$ pairs through this channel were found analytically in [9]. The calculation details are shown in Supplemental Material [10]. To obtain their numerical values, we pair this analysis with the solar temperature and density profiles of [11]. For the crude estimates in this Letter, we will use the following values of $\dot{n}$ at the center of the Sun and the χ production luminosity

$$\dot{n}_c \equiv \dot{n}(r=0) \sim 2 \times 10^9 \left(\frac{\epsilon}{10^{-15}}\right)^2 \left(\frac{\alpha_D}{1}\right) \text{cm}^{-3}\,\text{s}^{-1}, \quad (2)$$

$$L_\chi \equiv \int_{V_\odot} \dot{Q}dV \sim 8 \times 10^{36} \left(\frac{\epsilon}{10^{-15}}\right)^2 \left(\frac{\alpha_D}{1}\right) \text{MeV}\,\text{s}^{-1}. \quad (3)$$

If the χ electric charge ϵg_D is too large, the χ particles produced in stars carry away anomalously large amounts of energy thereby changing the evolutionary history of the stars. Bounds from the nonobservation of such an anomalous evolution in red giants sets the most stringent stellar bound on the χ electric charge [12]:

$$\epsilon \alpha_D^{1/2} \lesssim 2 \times 10^{-15} \quad (4)$$

Self-thermalization.—The initial population of χ particles produced in the Sun is in a state far from (local) thermal equilibrium. Here, we work out a sufficient condition for these particles to achieve thermalization.

The newly pair-created χ particles from plasmon decays in the Sun have a "hard" energy spectrum, with a typical energy E_{hard} roughly given by the temperature at the core of the Sun ($T_\odot$)

$$E_{\text{hard}} \sim T_\odot \sim 1 \text{ keV}. \quad (5)$$

Conservatively, we start with the lowest possible abundance of these hard particles arising from the free-streaming regime. Since these particles are produced relativistically, they typically stay inside the *solar core radius* r_{core}, which we take as $r_{\text{core}} \approx 0.2 r_\odot$ [13], for a period of $\sim r_{\text{core}}$. Hence, their starting number density is

$$n_{\text{hard}} \sim \dot{n}_c r_{\text{core}} \sim 8 \times 10^8 \left(\frac{\epsilon}{10^{-15}}\right)^2 \left(\frac{\alpha_D}{1}\right) \text{cm}^{-3}. \quad (6)$$

These E_{hard} and $n_{\text{hard}} \ll E_{\text{hard}}^3$ are a much higher average energy and a much lower number density compared to their would-be thermal equilibrium values for the same energy density. In order to thermalize, these particles must

decrease their average energy and increase their number density.

The high-energy, underoccupied initial state of the χ particles produced in the Sun in our scenario resembles that of the products of perturbative inflaton decay in the early Universe, a well-studied scenario [14–16]. The subsequent thermalization of such particles proceeds dominantly through inelastic processes. While kinematics forbids a single χ particle from spontaneously emitting a dark photon γ_D, particle production instead proceeds through bremsstrahlung. The rate of such a $2 \to 3$ process is roughly the rate of the enabling soft scattering process $\Gamma_{2\to2}^{\text{soft}}$ multiplied by a factor of α_D for the γ_D emission. Despite the extra α_D suppression, the rate $\Gamma_{2\to3}$ is enhanced due to the fact that it is dominated by soft momentum exchanges, whose cross section is large. This rate $\Gamma_{2\to3}$ is also limited by the formation time of the emitted γ_D, i.e., the so-called Landau-Pomeranchuk-Migdal (LPM) effect [17,18], but even so it is still much faster than other effects, such as the large-angle elastic scattering rate $\Gamma_{2\to2}^{\Delta\theta\sim1}$.

The soft $2 \to 2$ scattering rate is infrared divergent and given by

$$\Gamma_{2\to2}^{\text{soft}} \sim \frac{\alpha_D^2 n_{\text{hard}}}{q_{\min}^2} \sim \alpha_D E_{\text{hard}}, \quad (7)$$

where $q_{\min}$ is the IR cutoff of the dark photon momentum, which in our setup is set by the prethermalization dark-sector Debye scale $q_{\min} \sim \omega_D^{\text{pre}} \sim (\alpha_D n_{\text{hard}}/E_{\text{hard}})^{1/2}$ [19,20]. A χ particle with an incoming momentum $p_{\text{in}} \sim E_{\text{hard}}$ can scatter with another χ particle, become off-shell, and emit an extra γ_D with a momentum $k \lesssim p_{\text{in}}$. The rate for such a $2 \to 3$ process is given by [21]

$$\Gamma_{2\to3} \sim \alpha_D \min\left(\Gamma_{2\to2}^{\text{soft}}, t_{\text{form}}^{-1}\right), \quad (8)$$

where t_{form}^{-1} sets an upper bound on the splitting rate due to the fact that only one dark photon can be emitted in the timescale $t_{\text{form}} \sim \sqrt{E_{\text{hard}}^2/\alpha_D^2 n_{\text{hard}} k}$ it takes to resolve the dark photon [21–23]. This leads to a suppression of the splitting rate known as the LPM effect. It can be checked that $t_{\text{form}}^{-1} \lesssim \Gamma_{2\to2}^{\text{soft}}$ as long as $k \lesssim (E_{\text{hard}}^3/n_{\text{hard}})E_{\text{hard}}$. Since $E_{\text{hard}}^3 \gg n_{\text{hard}}$ [cf. Eqs. (5) and (6)] and the momentum of the emitted γ_D is kinematically limited to $k \lesssim E_{\text{hard}}$, the LPM effect is always important in the prethermalization stage, i.e., $\Gamma_{2\to3}$ is always set by the reciprocal formation time $t_{\text{form}}^{-1} \propto \sqrt{k}$. This process is therefore fastest for γ_D emissions with the largest momenta, $k \sim E_{\text{hard}}$, which boils down to the rate being $\Gamma_{2\to3} \sim \alpha_D^{3/2} \omega_D^{\text{pre}}$. In the subsequent $2 \to 3$ splittings, E_{hard} goes down, n_{hard} goes up, $k_{\min}$ goes up, which means $\Gamma_{2\to3}$ will keep increasing. Through processes such as $\gamma_D \chi \to \bar{\chi}\chi\chi$, the abundance of χ pairs increases with the abundance of the dark photons γ_D leading to an acceleration to thermal equilibrium in the

dark sector. Hence, the bottleneck lies in the beginning and the requirement for achieving thermalization with this process is $\Gamma_{2\to3}^{\text{initial}} r_{\text{core}} \gtrsim 1$, or

$$\epsilon \alpha_D^{5/2} \gtrsim 2 \times 10^{-26}. \tag{9}$$

Dark solar wind.—If the dark sector particles manage to completely self-thermalize, their mean free path would generically be far smaller than the length scales that dictate their collective macroscopic dynamics [24]. In that limit, such particles behave like a perfect fluid whose properties can be described in a largely model-independent way. Given the billion-year age of the Sun, it is likely that this fluid has relaxed by now to a steady state, described by the following time-independent energy and momentum equations [25]:

$$\frac{1}{r^2} \partial_r[r^2 \gamma^2 v(\tilde{\rho} + \tilde{p})] = \dot{Q}, \tag{10}$$

$$\frac{1}{r^2} \partial_r[r^2 \gamma^2 v^2(\tilde{\rho} + \tilde{p})] = -\partial_r \tilde{p}, \tag{11}$$

where r is the radial position with respect to the center of the Sun, $\gamma = (1 - v^2)^{-1/2}$ is Lorentz factor associated with the radial bulk velocity v of the fluid, $\tilde{\rho}(r)$ and $\tilde{p}(r)$ are the comoving density and pressure of the fluid, and $\dot{Q}(r)$ is the power per unit volume injection from the Sun in the form of $\chi\bar{\chi}$ pairs. Quantities with a tilde ˜ on top of it are defined in the rest frame of the fluid and those without it are defined in Sun's frame.

For simplicity, we assume here that the χ particles are massless or sufficiently light that they are adequately described as a radiation-dominated fluid with $\tilde{\rho} = 3\tilde{p} = a\tilde{T}^4$, with a a constant. Integrating the energy equation (10) gives us the comoving temperature $\tilde{T}$ of the fluid in terms of the fluid velocity v

$$\frac{4a}{3} \tilde{T}^4 = \frac{\int_0^r \dot{Q}(r')4\pi r'^2 dr'}{4\pi \gamma^2 v r^2}. \tag{12}$$

Substituting the above into the momentum equation (11) results in an equation for the fluid velocity only

$$\left(\frac{1/3 - v^2}{1/3 + v^2}\right) \frac{\partial \ln v}{\partial \ln r} = f(r) - \frac{2(1 - v^2)}{1 + 3v^2}, \tag{13}$$

where we defined a source function

$$f(r) \equiv \frac{\dot{Q}(r)r^3}{\int_0^r \dot{Q}(r')r'^2 dr'}. \tag{14}$$

The first term on the right-hand side of (13) is due to the energy injection (i.e., inertia injection) from the Sun, while the second term stems from the pressure gradient of the

fluid. Since the source $\dot{Q}(r)$ enters only via the dimensionless quantity $f(r)$, the resulting velocity profile $v(r)$ does not depend on the normalization of $\dot{Q}$, but only on the radial variation of the quantity $f(r)$. In particular, for the model (1) under consideration $f(r)$ is independent of both ϵ and α_D.

In order to solve (13) we need to specify some boundary conditions. Since the Sun produces χ particles with no net radial momenta to begin with, v must vanish at the origin. As we go to larger radii, there are two possible types of profiles, depending on whether or not v goes above the speed of sound $c_s = 1/\sqrt{3}$ during the outflow. Subsonic solutions (this includes hydrostatic solutions), where $v < c_s$ all the way, predict $v \propto r^{-2}$ at large distances from the Sun which, in turn, implies a nonzero comoving temperature $\tilde{T}$ at infinity through (12). However, the latter boundary condition is unphysical. Unless we add new ingredients to the model that provide pressure support on the fluid far from the Sun, e.g., through the high cosmic abundance of some particles interacting with the fluid, we expect $\tilde{T}$ to vanish at large r. This leaves us with the remaining possibility, namely the transonic solution, in which case the fluid velocity increases from subsonic speeds ($v < c_s$) at small r through the *sonic point* ($v = c_s$) to supersonic speeds ($v > c_s$) at large r. The monotonically increasing velocity implies a monotonically decreasing $\tilde{T}$, thus satisfying the vanishing $\tilde{T}$ boundary condition at infinity.

The sonic point ($v = 1/\sqrt{3}$) can be crossed smoothly only if it coincides with the zero of the right-hand side in (13) for $v = 1/\sqrt{3}$. The latter most likely occurs at around the Sun's core radius r_{core}, where $\dot{Q}$ starts to drop rapidly, and numerically we found it to lie at $r = r_{\text{sonic}} \approx 0.24\ r_\odot$. Thus, we require

$$v = \frac{1}{\sqrt{3}} \quad \text{at } r = r_{\text{sonic}} \approx 0.24\ r_\odot. \tag{15}$$

This completes the boundary conditions for numerically solving the velocity equation (13). We plot the resulting transonic Lorentz factor profile $\gamma(r)$, together with the source function $f(r)$, and the comoving fluid temperature $\tilde{T}$ from (12) in Fig. 1. It shows that beyond the sonic point $r \gtrsim r_{\text{sonic}}$ the Lorentz factor γ of the fluid flow asymptotes toward the well-known fireball solution [32], $\gamma \sim r/r_{\text{sonic}}$, for an adiabatically expanding fluid. In fact, as shown in Ref. [32], when $\gamma \gg 1$ the fireball solution $\gamma \sim r/r_{\text{sonic}}$ solves not only the sourceless $\dot{Q} = 0$ steady-state fluid equations (10) and (11) but also the time-dependent fluid equations. Thus, we expect $\gamma \sim r/r_{\text{sonic}}$ to hold robustly outside the Sun even if for some reason the fluid flow deviates from the assumed steady-state solution inside the Sun.
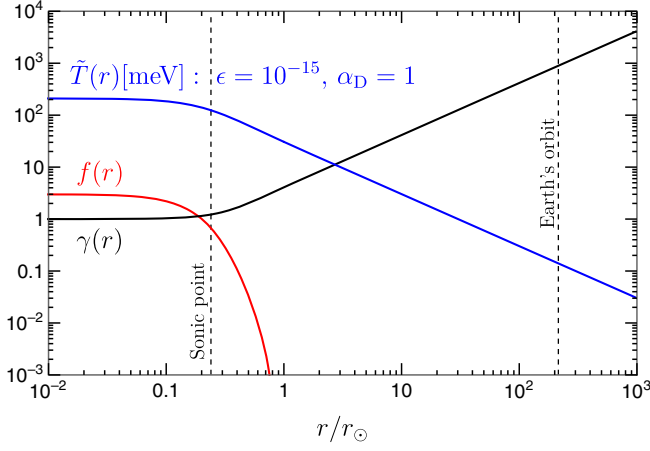
FIG. 1. Dark solar wind profiles as a function of the radial distance r from the Sun. The Lorentz factor $\gamma(r)$ solves the fluid velocity equation (13) with the transonic boundary condition (15). The source function $f(r) \equiv \dot{Q}(r)r^3/\int_0^r \dot{Q}(r')r'^2 dr'$ is computed with the millicharged-particle energy density injection rate $\dot{Q}$ of [9] and the numerical solar profiles of [11]. Both $\gamma(r)$ and $f(r)$ are independent of ϵ and α_D. The comoving temperature $\tilde{T}(r) \propto (\epsilon^2 \alpha_D)^{1/4}$ of the fluid is evaluated from the integrated energy equation (12) for $\epsilon = 10^{-15}$ and $\alpha_D = 1$. Also shown are the location of the sonic point, $r = 0.24\, r_\odot$, and Earth's orbit radius, $r = 215\, r_\odot$.

The structure of the fluid equation (13) considered here and the singling out of the transonic solution are mathematically analogous to that of Parker's solar wind [2] (see also Bondi accretion [33]). However, the physical mechanisms behind them are completely different. Parker's solar wind is isothermal, nonrelativistic, and accelerated by an interplay between pressure gradient and gravity. On the other hand, the dark solar wind is adiabatic, relativistic, and accelerated by an interplay between the pressure gradient and energy(inertia) injection from the Sun.

Properties near Earth.—As the flow expands to larger r and accelerates to higher Lorentz factors γ, the comoving temperature of the fluid $\tilde{T}$ cools down adiabatically according to (12). The integral in (12) for $r \gtrsim r_{\text{core}}$ yields the luminosity L_χ of the χ particles produced in the Sun, resulting in $(4a/3)\tilde{T}^4 \approx \gamma^{-2}(L_\chi/4\pi r^2)$ for $v \approx 1$. Interestingly, in the highly relativistic limit $\gamma \gg 1$ expected at $r \gg r_{\text{sonic}}$ the scalings with r of the average energy per particle $\langle E \rangle \sim \gamma\tilde{T} \approx$ const and number density $n \sim \gamma\tilde{T}^3 \propto r^{-2}$ in the Sun's frame are identical to those in the free streaming case, i.e., it is as if these particles simply free streamed from the surface at which the fireball approximation starts to hold ($r \sim r_{\text{sonic}}$). The latter is understandable because the acceleration of the fluid to relativistic bulk velocities manifests itself at the particle level as the velocities of the particles becoming increasingly radial the farther they are from the Sun (relativistic beaming).
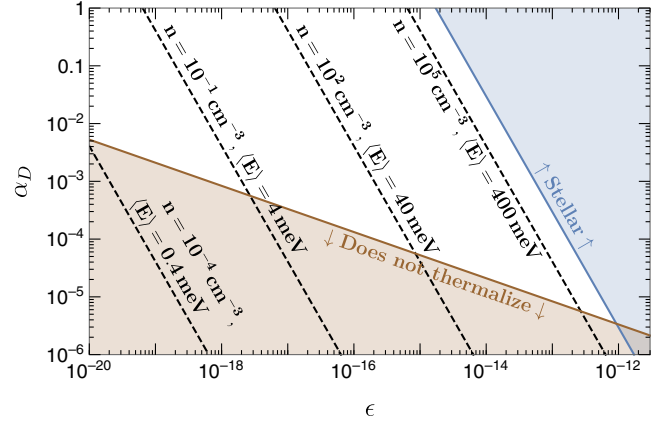
FIG. 2. Viable parameter space and predictions. The blue region violates the stellar cooling limit (4). The red region does not satisfy the thermalization requirement (9). The dashed lines correspond to different combinations of dark solar wind density n (21) and average energy per particle $\langle E \rangle$ (20) near Earth.

All things considered, the average energy $\langle E \rangle$ and number density n of the dark particles at $r \gg r_{\text{sonic}}$ in the Sun's frame are given up to O(1) factors by

$$\langle E \rangle \sim \left(\frac{L_\chi}{r_{\text{sonic}}^2}\right)^{1/4} \sim 1 \text{ eV} \left(\frac{L_\chi}{10^{-2}L_\odot}\right)^{1/4}, \quad (16)$$

$$n \sim \frac{n_{\text{FS}}\langle E \rangle_{\text{FS}}}{\langle E \rangle} \sim 10^3 n_{\text{FS}} \left(\frac{L_\chi}{10^{-2}L_\odot}\right)^{-1/4}. \quad (17)$$

By contrast, in the free-streaming case the average energy per particle is given by the core temperature of the Sun $\langle E \rangle_{\text{FS}} \sim \text{keV}$ and if these particles are massless energy conservation then gives $n_{\text{FS}} \sim L_\chi/r^2\langle E \rangle_{\text{FS}}$. When the dark particle luminosity saturates the cooling limit, $L_\chi \sim 10^{-2}\, L_\odot$, the dark solar wind gives $\sim 10^3$ lower average energy $\langle E \rangle$ and $\sim 10^3$ higher number density n_χ compared to those in the free-streaming case. The results in the two cases deviate even more for $L_\chi \ll 10^{-2}\, L_\odot$. For the dark fermion dark photon model (1) considered in this Letter, and with the O(1) factors included, the results at $r \gg r_{\text{sonic}}$ are

$$\gamma \approx 893 \left(\frac{r}{1 \text{ AU}}\right), \quad (18)$$

$$\tilde{T} \approx 0.14 \text{ meV} \left(\frac{\epsilon}{10^{-15}}\right)^{1/2} \left(\frac{\alpha_D}{1}\right)^{1/4} \left(\frac{1 \text{ AU}}{r}\right), \quad (19)$$

$$\langle E \rangle \approx 4\gamma\tilde{T} \approx 0.5 \text{ eV} \left(\frac{\epsilon}{10^{-15}}\right)^{1/2} \left(\frac{\alpha_D}{1}\right)^{1/4}, \quad (20)$$

$$n = \frac{5\zeta(3)}{\pi^2}\gamma\tilde{T}^3 \approx \frac{2 \times 10^5}{\text{cm}^3} \left(\frac{\epsilon}{10^{-15}}\right)^{3/2} \left(\frac{\alpha_D}{1}\right)^{3/4} \left(\frac{1 \text{ AU}}{r}\right)^2, \quad (21)$$

where we have used $\tilde{\rho} = a\tilde{T}^4$ with $a = (2 + 4 \times 7/8)(\pi^2/30)$ corresponding to dark photons and $\chi\bar{\chi}$ pairs in obtaining the above results, and $\langle E \rangle$ was found by averaging over all species using their spectra as seen on Earth (see Supplemental Material [10]). See Fig. 2 for the model predictions at different points in the parameter space.

Detection.—In principle, the dark photons as well as the dark fermions in the dark plasma can be detected. Since the prospects are futuristic, we only provide order-of-magnitude estimates and defer a systematic study for future work.

While the ultrarelativistic dark photons in the dark solar wind have suppressed absorption rates, the dark fermions can potentially be probed through their scattering with electrons in dark matter direct detection experiments. In elastic scattering, since the dark fermions have energies much lower than the mass of the electron, the energy deposited in the electron is suppressed. Inelastic processes wherein a bound electron is kicked out of its shell can kinematically permit the dark fermion to lose $\mathcal{O}(1)$ of its kinetic energy i.e., almost $\sim$eV. While these processes are kinematically more favorable, the cross-section for such inelastic processes is suppressed by the momentum transferred during the process, requiring detectors with larger target masses to probe phenomenologically interesting parts of parameter space. We discuss these possibilities in detail in future work.

The dark plasma flow studied here has properties that are very distinct from that of cold dark matter, permitting detection strategies beyond scattering in direct detection experiments. The unidirectional, relativistic, and strongly coupled nature of the flow may allow us to probe this parameter space through experiments in the same spirit as the so-called *direct deflection* [34,35]. The idea is to somehow perturb the dark plasma wind and measure its backreaction in the form of SM electric or magnetic fields downstream. The generically tiny dark Debye length of the dark plasma in our scenario quickly erases any static dark electric field in the dark plasma once it is removed from the perturber. However, dark electric currents may persist long enough to be detected [36]. It would be interesting to quantify this nontrivial dynamics with the help of numerical simulations.

Discussion.—We pointed out a new generic phenomenon, here referred to as *dark solar wind*, that arises in a generic light dark sector with sufficiently weak SM interactions to avoid stellar cooling limits and sufficiently strong, number-changing self-interactions to self-thermalize upon emission. Unlike in the free-streaming scenario, the solar emission in this regime is less energetic, denser, and behaves like a relativistically expanding fluid. Since the properties of this fluid are dictated by thermal-equilibrium and steady-state hydrodynamics, they are not sensitive to the details of the underlying microphysics. We considered dark fermions charged under a dark photon that kinetically mixes with the SM photon as an example, spelled out a sufficient condition for achieving thermalization in the dark sector, numerically solved the hydrodynamic equations for the resulting fluid, and worked out their properties on Earth or elsewhere in the solar system.

Though we assumed that the dark fermion χ is massless in our discussions, they are still valid for nonzero but light enough dark fermion mass m_χ. The thermalization condition is unaffected as long as m_χ is less than the lowest relevant energy scale, namely the prethermalization Debye frequency ω_D^{pre}, while the fluid dynamics is unchanged as long as the dark fermions remain relativistic, i.e., $m_\chi \ll \tilde{T}$, up to the radius of interest. As we increase m_χ from zero, we cross ω_D^{pre} way before the comoving temperature near Earth $\tilde{T}(r = 1 \text{ AU})$. We discuss this regime where the thermalization condition is parametrically different but the fluid dynamics and hence the model predictions are unchanged in Supplemental Material [10]. We leave the explorations of yet higher m_χ regime as well as the effects of a nonzero dark photon mass for future work.

*jaechang@umd.edu
†david.kaplan@jhu.edu
‡srajend4@jhu.edu
§hramani@stanford.edu
‖etanin1@jhu.edu

[1] G. G. Raffelt, Phys. Rep. **198**, 1 (1990).
[2] E. Parker, Space Sci. Rev. **4**, 666 (1965).
[3] B. Holdom, Phys. Lett. **166B**, 196 (1986).
[4] J. Alexander *et al.*, arXiv:1608.08632.
[5] M. Battaglieri *et al.*, in U.S. Cosmic Visions: New Ideas in Dark Matter (2017), arXiv:1707.04591.
[6] A. Arvanitaki, S. Dimopoulos, M. Galanis, D. Racco, O. Simon, and J. O. Thompson, J. High Energy Phys. 11 (2021) 106.

[7] C. Dvorkin, T. Lin, and K. Schutz, Phys. Rev. D **99**, 115009 (2019).

[8] A. Mathur, S. Rajendran, and E. H. Tanin, Phys. Rev. D **102**, 055015 (2020).

[9] J. H. Chang, R. Essig, and A. Reinert, J. High Energy Phys. 03 (2021) 141.

[10] See Supplemental Material at http://link.aps.org/supplemental/10.1103/PhysRevLett.129.211101 for a review of plasma effects in the Sun, the local energy spectra of dark solar wind particles, and a discussion on dark sector thermalization in the case of massive dark fermions.

[11] J. N. Bahcall, A. M. Serenelli, and S. Basu, Astrophys. J. Lett. **621**, L85 (2005).

[12] H. Vogel and J. Redondo, J. Cosmol. Astropart. Phys. 02 (2014) 029.

[13] Note that the SM plasma, and hence $\dot{n}$, is roughly uniform within the Sun's core radius $r_{core} \approx 0.2 \, r_\odot$ and decays rapidly outside of it. For this reason it is more appropriate to use r_{core} instead of the full solar radius $r_\odot$ in our estimates.

[14] S. Davidson and S. Sarkar, J. High Energy Phys. 11 (2000) 012.

[15] K. Harigaya and K. Mukaida, J. High Energy Phys. 05 (2014) 006.

[16] K. Mukaida and M. Yamada, J. Cosmol. Astropart. Phys. 02 (2016) 003.

[17] P. B. Arnold, G. D. Moore, and L. G. Yaffe, J. High Energy Phys. 11 (2001) 057.

[18] A. Kurkela and G. D. Moore, J. High Energy Phys. 12 (2011) 044.

[19] M. E. Carrington, D.-f. Hou, and M. H. Thoma, Eur. Phys. J. C **7**, 347 (1999).

[20] P. B. Arnold, G. D. Moore, and L. G. Yaffe, J. High Energy Phys. 01 (2003) 030.

[21] M. Garny, A. Palessandro, M. Sandora, and M. S. Sloth, J. Cosmol. Astropart. Phys. 01 (2019) 021.

[22] S. Peigne and A. V. Smilga, Phys. Usp. **52**, 659 (2009).

[23] The formation time t_{form} can be defined as the time it takes for the emitted dark photon to acquire a phase difference $\Delta\phi = O(1)$ along the worldline of the emitting χ particle. A derivation of t_{form} in our context, as well as the justifying assumptions, can be can be found in Supplemental Material [10].

[24] This is trivially satisfied for the model (1) we are considering if the condition (9) is met. More specifically, we have checked *a posteriori* that the mean free time of the dark particles as seen in the Sun's frame is easily much smaller than the timescale for, e.g., the density of particles to change by an O(1) factor due to the fluid expansion.

[25] Numerical simulations [26,27] of analogous systems [2,28–31] suggest that the steady state solution is an attractor and the relevant relaxation timescale is given by the hydrodynamical timescale, which for our solar system is roughly the flow time to 1 AU, namely ∼10 min.

[26] R. F. Stellingwerf and J. Buff, Astrophys. J. **221**, 661 (1978).

[27] E. R. Keto, Mon. Not. R. Astron. Soc. **493**, 2834 (2020).

[28] A. R. Garlick, Astron. Astrophys. **73**, 171 (1979).

[29] J. A. Petterson, J. Silk, and J. P. Ostriker, Mon. Not. R. Astron. Soc. **191**, 571 (1980).

[30] T. Theuns and M. David, Astrophys. J. **384**, 587 (1992).

[31] A. K. Ray and J. K. Bhattacharjee, Phys. Rev. E **66**, 066303 (2002).

[32] T. Piran, A. Shemi, and R. Narayan, Mon. Not. R. Astron. Soc. **263**, 861 (1993).

[33] H. Bondi, Mon. Not. R. Astron. Soc. **112**, 195 (1952).

[34] A. Berlin, R. T. D'Agnolo, S. A. R. Ellis, P. Schuster, and N. Toro, Phys. Rev. Lett. **124**, 011801 (2020).

[35] A. Berlin and K. Schutz, Phys. Rev. D **105**, 095012 (2022).

[36] G. Baym, D. Bodeker, and L. D. McLerran, Phys. Rev. D **53**, 662 (1996).